UNIVERSITÉ BORDEAUX 1 Sciences Technologies
MATMECA
Ecole d'Ingénieurs en Modélisation Mathématique et Mécanique
UCL

MODELLING OF GUIDED ULTRASONIC WAVES PROPAGATING ALONG A STIFFENER BONDED TO A PLATE
&
RESEARCH INTO ULTRASONIC HORN

Project of Thomas LEMONNIER

Supervised by
Dr. Paul Fromme
Dr Nader Saffari

London

Summer 2008

PREFACE

This project was made at the University College London between June and August 2008. My best thanks go to Dr. Paul Fromme and Dr. Nader Saffari, my tutors, who made it possible for me to go abroad for my work placement which allows me to improve my English and also to learned new knowledge in Physics. It was a great experience to see how researchers work and well to live in London.

Moreover, I'm very thankful to Eric Kostson, a PhD student of Dr. Fromme who explained to me many concepts about the study of propagating waves. We had many interesting discussions about propagating waves and also about English language and football.

To conclude, I hope that Dr Paul Fromme and Dr Nader Saffari were happy with me because I was very happy to work with them, it was a very interesting project. I learned many interesting thing about wave propagation, a theme I didn't work or study before this internship.

TABLE OF CONTENTS

PART 1

MODELLING OF GUIDED ULTRASONIC WAVES PROPAGATING ALONG A STIFFENER BONDED TO A PLATE

I. INTRODUCTION

Engineering structures, e.g. aircraft, are subject to loads during service which can cause damage. Non-destructive methods such as ultrasonic testing (UT) have been developed to detect the presence of damage, e.g., cracks. However, classical UT methods scan through the thickness of the structure, which can pose problems in structures with limited access. Therefore guided ultrasonic waves are investigated for the detection of defects as they propagate over larger distance in structures with limited access.

For complex structures, the wave propagation can not be described analytically. Therefore, to understand the wave propagation in complex structures, Finite Element Analysis (FEA) is used.

During this project, the guided ultrasonic wave propagation in a three-dimensional model of a stiffener bonded to a plate has been studied using the software ABAQUS.

II. WAVES IN PLATE

This first chapter presents the approach used to understand guided ultrasonic wave propagation and to check the results for a simple plate structure against theoretical calculations.

1. Propagation of the antisymmetric mode A0 and the symmetric mode S0.

The idea is to work at a low frequency where only the fundamental modes A0 and S0 can propagate in an infinite plate. The theoretical dispersion relations for a traction-free plate show that above a certain *fd* (frequency x thickness) others mode exist and propagate.

The phase velocity and wave number for the fundamental modes can be calculated theoretically and compared to simulation results to check the accuracy of the FE model.

ABAQUS models are generally created using ABAQUS CAE that provides a graphical interface for creating and submitting simulations. However, ABAQUS CAE does not support all options that ABAQUS provides. More options and better control are available using an input file. In a previous MSc project, models for the simulation of guided wave propagation in a simple steel plate were set-up by Robert Watson[2], creating input files using MATLAB.

The geometry of the simple system is presented in Fig. 1. The aluminium plate has a thickness equal to 6 mm and it is 1000 mm long and 40 mm wide.

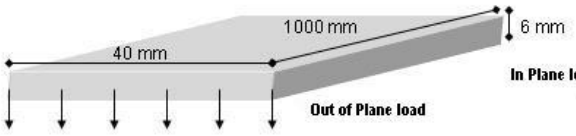

Figure 1 – left : Direction of the load to obtain the antisymmetric mode A0

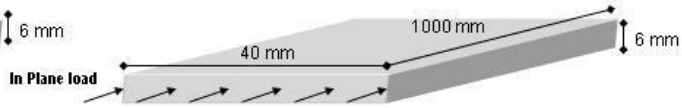

Right : Direction of the load to obtain the first symmetric mode S0

Boundary conditions are used on each side of the plate to avoid the generation of width modes. Horizontal displacements are restricted for all points on the side of the plate to model an infinite plate.

The excitation signal consists of a 5 cycle toneburst with a centre frequency of 100 kHz (fd = 0.6 MHz mm). Fig 1 shows how the plate must be excited to obtain the different modes. Monitoring points are placed in the middle thickness (Fig. 2) of the plate and positioned along the length of the model. Other monitoring points are placed across the thickness (Fig. 2) to monitor the mode shape of the ultrasonic wave. Explicit time integration is used and the element size ($\Delta x, \Delta y, \Delta z = 1mm$) and time step ($\Delta t = 1.E-07$ s) are picked to adhere to the usual stability criteria: $\max(\Delta x, \Delta y, \Delta z) < \frac{\lambda}{8}$

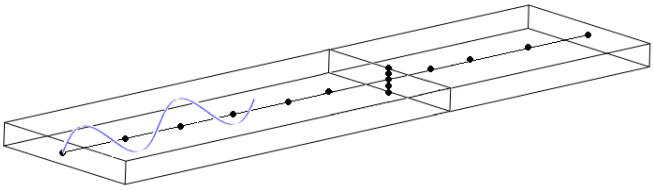

Figure 2. – Placement of monitoring points

First simulations were done using an excitation force. However, a tail appeared at the end of the signal which is incorrect. A solution was found by applying the excitation signal as a displacement (using the Boundary Condition command in ABAQUS).

The calculated results presented in appendix A show that the simulation is in accordance with the theory, modeshapes, wavenumber and frequency are correct.

2. Combined propagation of the antisymmetric and symmetric mode.

The second part of this first study is about the propagation of a wave created by a combined load (Fig. 3) to excite the antisymmetric and symmetric modes simultaneously. This simple case is useful to study because only two modes propagate.

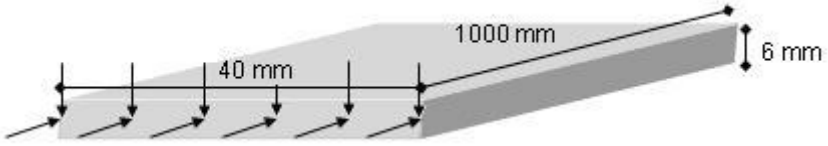

Figure 3. – Geometry and loading direction to obtain the combined antisymmetric and symmetric mode

Fig 4. is a simple screenshot from ABAQUS, which shows the difference in velocity between the two modes.

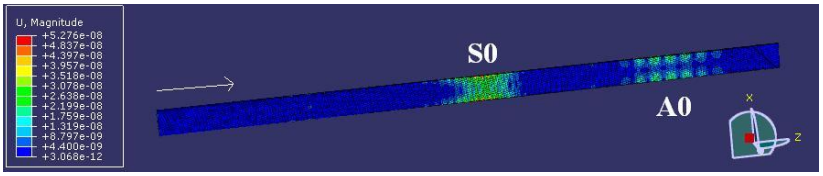

Figure 4 - ABAQUS pictures of the aluminium plate at 0.25 ms

The 2D-FFT of the out-of-plane displacement coupled to the in-plane is shown Fig. 5. Extracting the maxima for each frequency the lines can be compared against theoretical calculations. Good agreement for the S0 mode and the A0 mode can be seen Fig. 6.

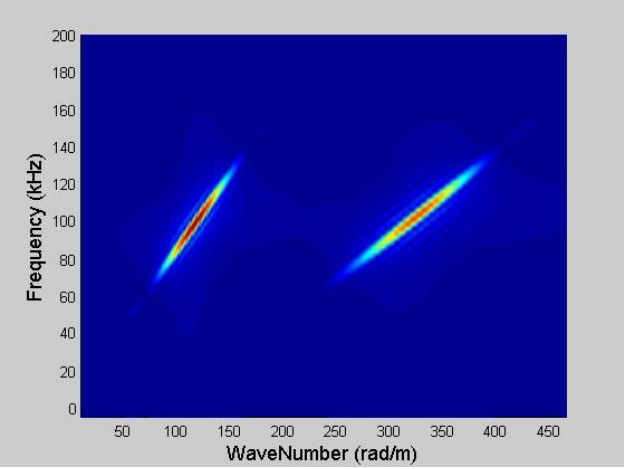

Figure 5 – 2DFFT for the simulation with in-plane and out-of-plane displacement

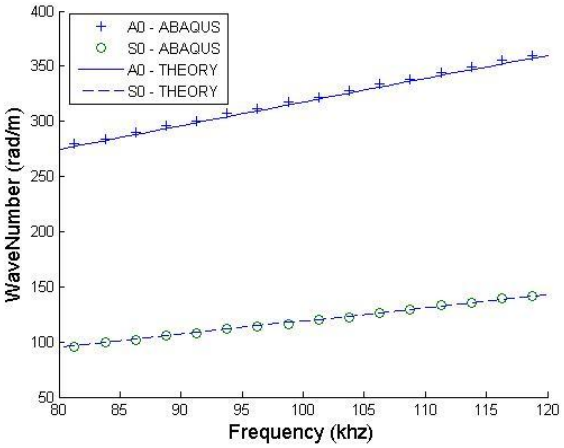

Figure 6 – Wavenumber against frequency for the simulation with in-plane and out-of-plane displacement

3. Damping Influence

For the following study, the wave propagation along a stiffener bonded to a plate, the introduction of the damping effect is necessary. The adhesive bond and the viscoelastic Perspex plate have a significant damping effect[4] on the propagating waves. However, there are different solutions to realise damping with ABAQUS. The solution chosen is the one used in the Master-project of Jonas Wyrsch[5] were the ABAQUS function damping was used.

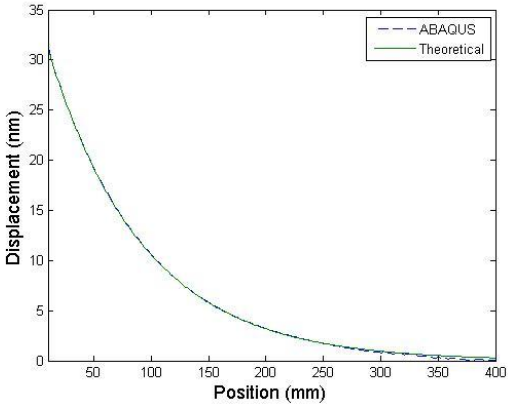

Figure 7 – Out-of-plane displacement in plate with damping (blue : ABAQUS, green : theoretical)

In ABAQUS, Rayleigh damping can be applied by defining values for the two damping factors α and β. It is assumed that α is negligible in the ultrasonic range and that β, the stiffness proportional Rayleigh damping factor, is approximated by: $\beta \approx \frac{E''}{\omega E'}$

Where ω is the angular frequency, E' the storage modulus and E'' the loss modulus in the expression: $E^* = E' + iE''$ for the complex elastic modulus.

To measure the damping phenomenon a load is applied as in Fig 1 (right). Monitoring points are placed in the middle of the plate. Fig. 7 shows the value of the in-plane displacement at different distances. The theoretical curve is calculated from the attenuation coefficient of 0.273 dB/λ (decibel/wavelength). The damping phenomenon can be seen from the decrease in amplitude and it shows that the ABAQUS function damping is a good way to implement damping.

III. WAVE PROPAGATION ALONG A STIFFENER BONDED TO A PLATE

1. Creation and properties of the model

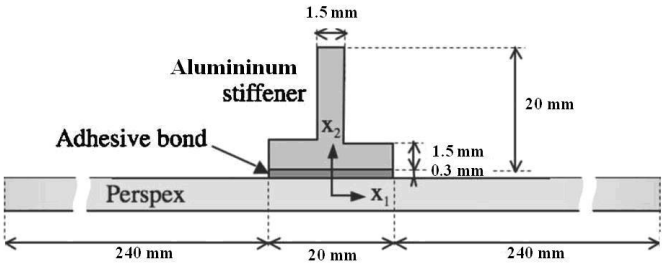

Fig. 8 – Schematic of an aluminium stiffener bonded to a Perspex plate

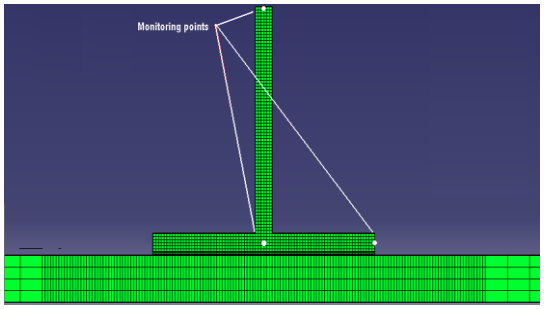

Fig. 9 – ABAQUS picture of the model

The geometry of the problem is shown in Figure 8. The plate is made of Perspex and has a thickness equal to 3.8 mm. Material properties are given in Table 1. The stiffener has a T-shape and it is made of aluminium. A 0.3-mm-thick layer of adhesive is present between the plate and the stiffener. The aim of this part is to monitor bond quality of adhesive using guided ultrasonic wave propagating along the stiffener.

	Plate	Bond	Stiffener
Size	400mm*500mm*3.8mm	400mm*20mm*0.3mm	400mm*20mm*20mm
Material	Perspex	Adhesive	Aluminium
Properties	E=4.05 GPa, v=0.35, β=0.1 μs	E=0.45 GPa, v=0.46, β=0.3 μs	E=67.6 GPa, v=0.353

Table 1 – Mechanical properties

The ABAQUS input file is created using Matlab and imported into ABAQUS. The element sizes are given in Table 2, note that the Perspex plate is composed of 2 parts (Fig. 9): one with Δx = 2 mm and one with Δx = 0.25 mm. Continuity of displacement and stresses are imposed at the internal borders between the stiffener, the adhesive layer and the Perspex plate. Stress-free conditions are defined at all outer limits of the system.

	Δx (mm)	Δy (mm)	Δz (mm)
Stiffener	0.25	0.25	2
Adhesive	0.25	0.1	2
Plate	0.25 – 2	0.95	2

Table 2 – Elements size of geometry used in models

2. Comparison between two excitations

The first study proposed by Dr Paul Fromme was to apply two different excitations to see which modes are excited. The first excitation is a horizontal displacement on the whole face of the stiffener and the second one is a pressure only on one part of the stiffener (see Fig. 10).

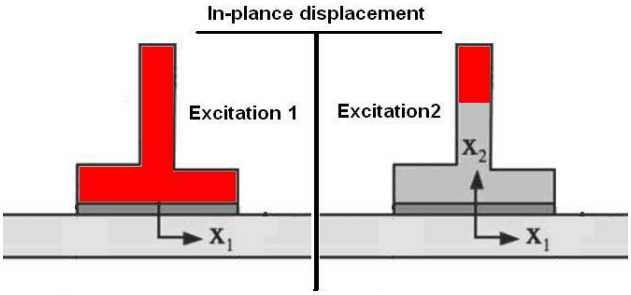

Fig. 10 – Schematic of the two different excitation used in the study

As in the previous study, the main way to observe a difference between the propagating modes is the analysis of the 2D-FFT diagram. Fig. 11 shows the 2D-FFT for monitoring points on the middle of the stiffener. It can be seen from the figure that with excitation 2, more modes propagate along the stiffener than with excitation 1.

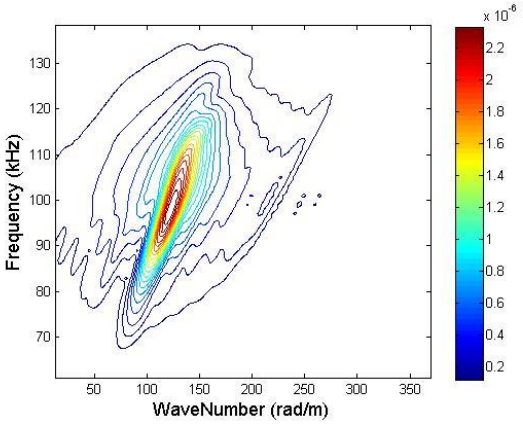

Figure 11.a - Excitation 1 - 2D FFT

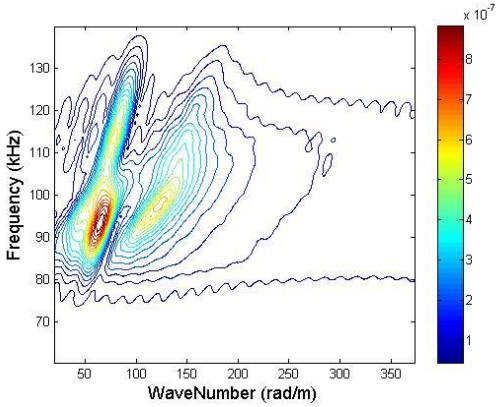

Figure 11.b - Excitation 2 - 2D FFT

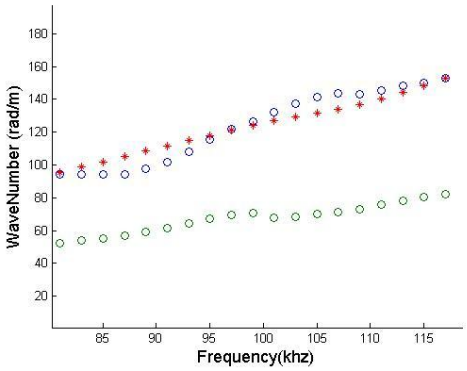

Figure 12.a - Dispersion curves for the two excitations (+-line: Excitation 1 / o-line: Excitation 2)

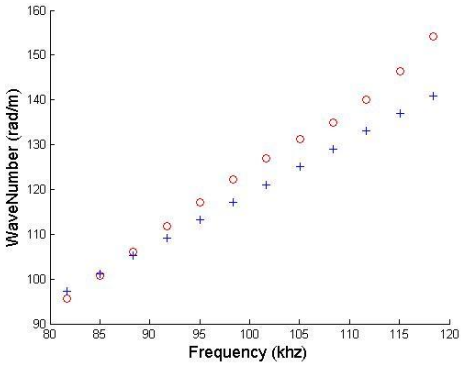

Figure 12.b - Dispersion curves(+-line: Excitation 1 / o-line: S0 mode in plate)

Moreover, Fig. 11 shows that the amplitude is bigger for the excitation 1 than for the excitation 2. In fact, it is normal because as fewer nodes are excited, less amplitude is expected. Figure 12.a shows that the excitation 1 produces one mode and the excitation 2 produces two modes. One of these modes seems to be the same for both excitations. Figure 12.b shows that the mode produced by excitation 1 is a S0 mode, the mode one would expect to be dominant for the excitation. The excitation 2 will be used for the next study because it is this excitation which will be used is the experiment.

3. Varying stiffness of adhesive layer

The propagation of energy in the model depends on the stiffness of the adhesive layer. If the adhesive is good the energy will propagate into the plate. Therefore, in this part three simulations are compared with different quality of the adhesive bond. The quality of the adhesive bond is partly given by the Young modulus of the adhesive, so this parameter changes in each simulation. Table 3 shows parameters for the adhesive bond for each simulation. In fact, only the Young's modulus changes, the rest kept constant.

Simulation 1	Simulation 2	Simulation 3
Properties: E=450 MPa, ν=0.46, β=0.3 μs	Properties: E=45 MPa, ν=0.46, β=0.3 μs	Properties: E=4.5 MPa, ν=0.46, β=0.3 μs

Table 3 – Mechanical properties

Figure 13 shows the time traces of a point in the middle of the stiffener at 100 mm from the load.. The result is not surprisingly: when the adhesive bond is good – simulation 1 – the amplitude is smaller than when the adhesive bond is bad – simulation 3. Figure 14 highlights the same phenomenon. A sort of energy is known by calculating the surface below the frequency curve contained in the stiffener for each position of a point on the top of the stiffener. It is obvious that when the adhesive is good, the energy well propagates into the Perspex.

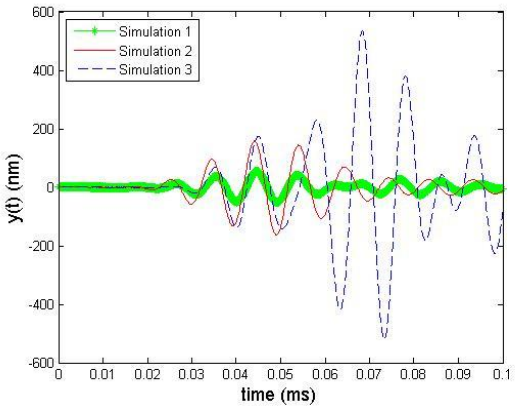

Figure 13. Time traces for the 3 different simulations.

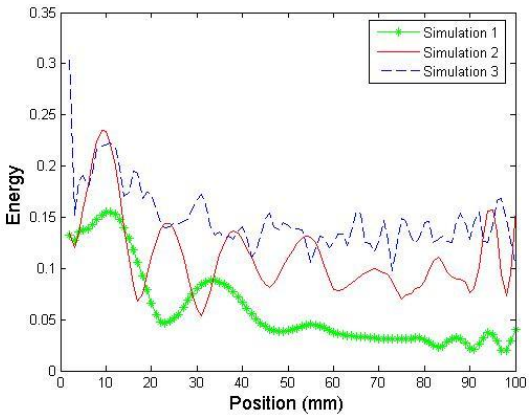

Figure 14. "Energy" contained on the stiffener for the 3 different simulations

Before studying the 2D-FFT, it is interesting to see the wavenumber curve at 100 kHz. This curve is done using the value of the 2D-FFT matrix and extracting the value for 100 kHz. Figure 15 shows, for a point in the middle of the stiffener (APPENDIX B), that the maxima of the wave number curve for each simulation are similar.

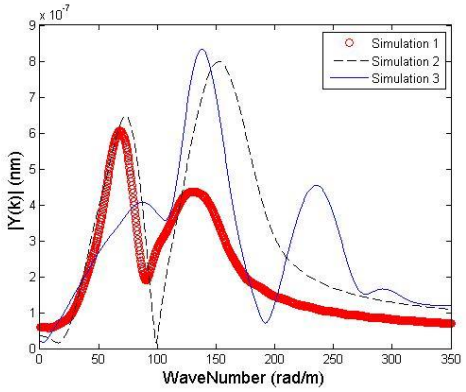

Figure 15. Wavenumber curve for the 3 different simulations

Simulation 1 : 68.54 rad/m - 130 rad/m
Simulation 2 : 73.26 rad/m - 152 rad/m
Simulation3 : 87 rad/m - 137 rad/m (236 rad/m)

Table 4 – Value of wavenumber at f=100 kHz.

To compare the different simulations, a 2D FFT (APPENDIX C) is used to see the different frequency which propagates into the stiffener.

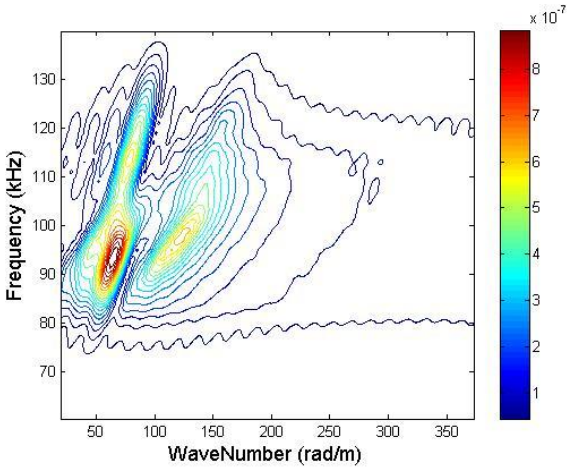

Figure 16.a - 2D FFT – Simulation 1

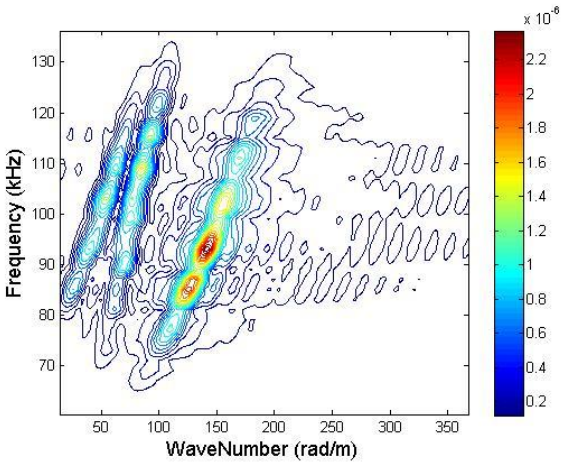

Figure 16.b - 2D FFT – Simulation 2

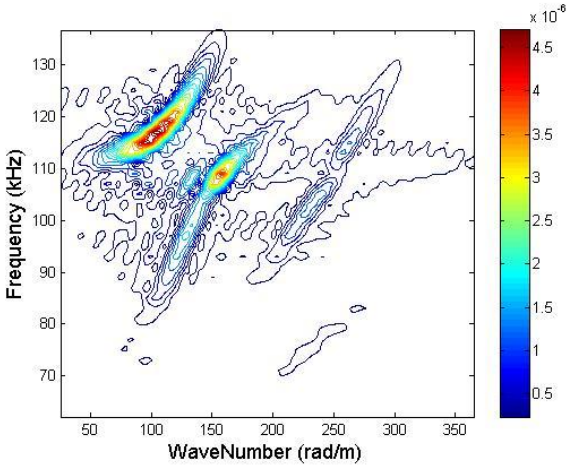

Figure 16.c - 2D FFT – Simulation 3

In figure 16, 2D FFT for monitoring points in the middle of the stiffener, highlight that the amplitude increase when the quality of the adhesive bond decreases. The number of modes is bigger for the simulation 3 because the wave only propagates into the stiffener and not into the Perspex plate which imply a lot of reflections. According to all figures 6 in Appendix C, it appears that the good bond is dominated by an S0-like-mode : for simulation 1, 2D-FFT for U2 and U3 displacement seems to be not very different. Moreover for simulation 2 it still be the same however it is not evident for simulation 3.

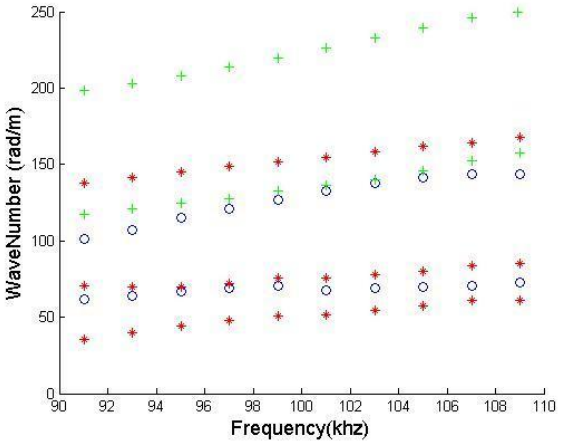

Figure 17 - Wavenumber against frequency for the 3 simulations
*(o-line: Simulation 1 / *-line: Simulation 2 / +-line: Simulation 3)*

Extracting the maxima for each frequency, figure 17 shows that 1 mode is similar for the three simulations. Moreover, between simulation 1 and simulation 2 one mode seems to be in common.

These results should be compared with semi-analytical finite element (SAFE) predictions to check the accuracy of the FE model and analysis. Even though only rather small changes in the wavenumbers are predicted, the amplitude of the excited modes seems to vary significantly depending on the bond quality.

The displacement of the stiffener at one location and time is displayed for the 3 different simulations. The mode shape for all 3 simulations looks similar as expected, different amplitudes are observed, which could be measured experimentally.

Modeshapes are not very different, the amplitude is different in accordance with the previous results (figure 13). However, to see the deformed shape for all the simulations, amplitudes are multiplied by a factor which is different.

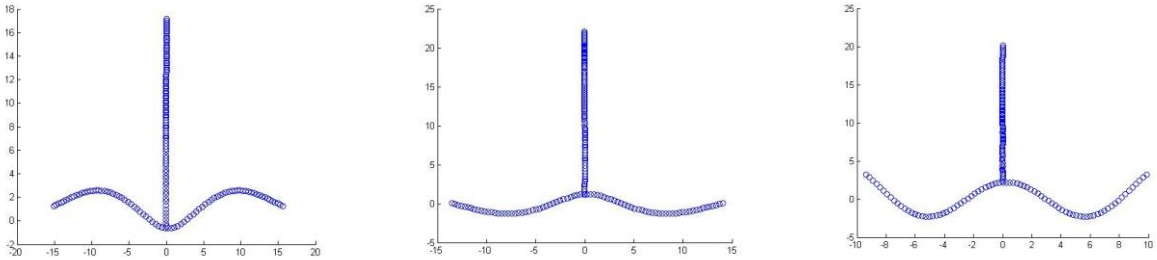

Simulation 1 Simulation 2 Simulation 3

Stiffener's modeshape – 400 micro sec

The main displacement seems to be in the lower part of the stiffener. Modeshapes look reasonably similar, which would mean that we see the same mode propagating.

4. Bibliography

[1] F. Yeo and P. Fromme *Guided ultrasonic wave inspection of corrosion at ship hull structures*Structures, 2006

[2] Watson, R.J., Modelling of Ultrasonic Wave Scattering at Defects, MSc Thesis, UCL, 2007

[3] Rose, J.L., Ultrasonic Waves in Solid Media, 1999

[4] http://www.ndted.org/EducationResources/CommunityCollege/Ultrasonics/cc_ut_index.htm (damping phenomenon)

[5] Wyrsch, J., Ultrasonic wave propagation in multilayered aircraft-structures, MSc Thesis, ETH Zurich / UCL, 2007

APPENDIX

A. WAVES IN PLATES: RESULTS

Here are results of the problem presented chapter I.

A.1. Modeshapes

To be sure that it is the ultrasonic wave we expect which is propagating along the plate, it is interesting to show modeshapes[3] which highlight symmetric and anti-symmetric phenomenon of each mode. Here, figure 3.a, it is possible to see that for the out-of-plane load, out-of-plane displacement is anti-symmetric and in-plane displacement is very small compared to out-of-plane displacement which is normal[3].

Out-of-plane load

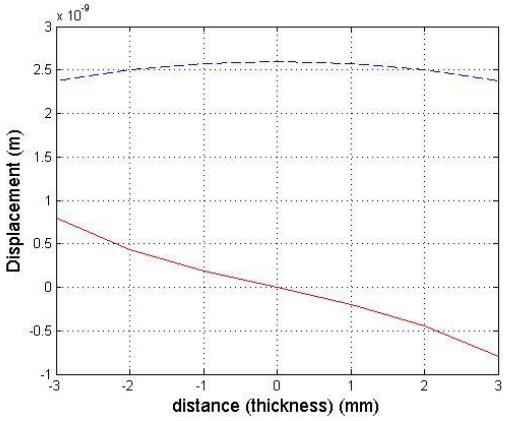

Figure I.a - In-plane / out-of-plane displacement

In-plane load

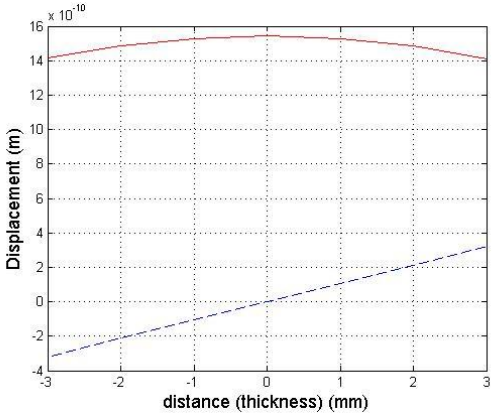

Figure I.b - In-plane / out-of-plane displacement

In-plane (dashed line) – Out-of-plane (solid line)

A.2. Time traces

Figures 4.a.b.c.d present time traces for in-plane and out-of-plane displacement which show that an A0 mode propagates along the plate when the load is out-of-plane and that a S0 mode propagates when the load is in-plane.

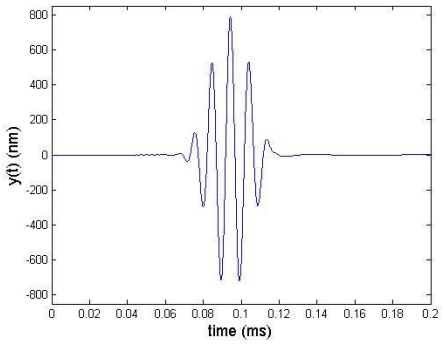

Figure II.a – Out-of-plane displacement for out-of-plane load

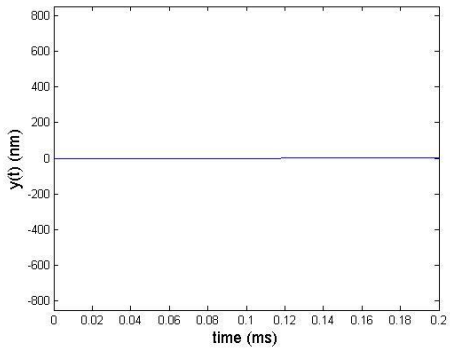

Figure II.c – Out-of-plane displacement for in-plane load

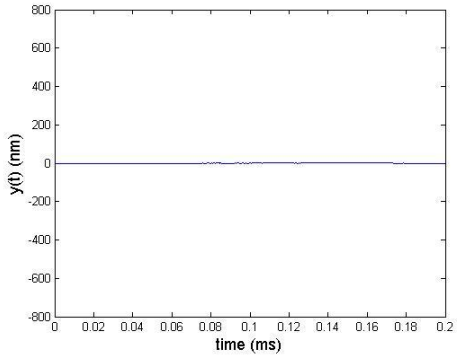

Figure II.b – In-plane displacement for Out-of-plane load

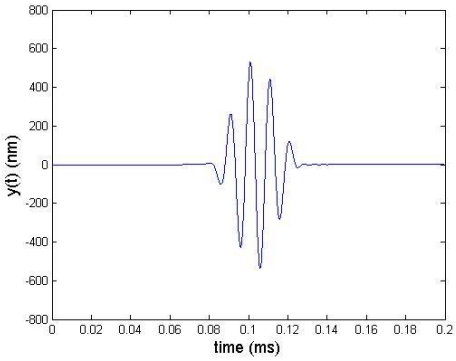

Figure II.d – In-plane displacement for In-plane load

A.3. Frequency curves

Figures 5.a and 5.b present time and frequency curves for the out-of-plane displacement for both modes. It confirms that the wave which propagates along the plate has a frequency of 100 kHz for both modes.

Out-of-plane load

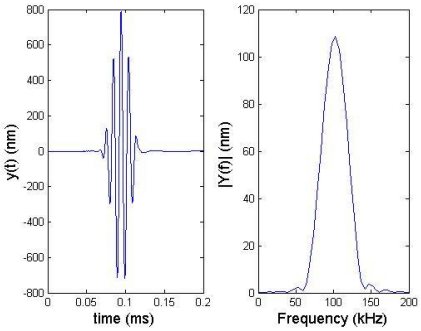

Figure III.a - Time and frequency curves for the out-of-plane displacement

In-plane load

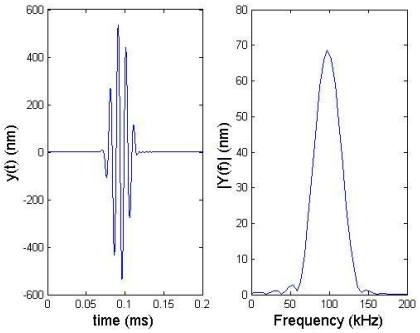

Figure III.b - Time and frequency curves for the in-plane displacement

A.4. Wavenumber curves

Figures 6.a and 6.b highlight the fact that the antisymmetric and the symmetric mode do have different wave number which corresponds to different waves' velocity. For the A0 mode, the wavenumber found is approximately 315 rad/m. However it is possible to calculate it analytically thanks to the phase velocity $k = \frac{\omega}{c_p}$. For the A0 mode, the phase velocity is 1977 m/s (theoretically) which implies that k=318 rad/m. Likewise, for S0 modes which phase velocity is 5277 m/s which implies k=119 rad/m, graphically k=120 rad/m, so results are in accordance with theory.

Out-of-plane load

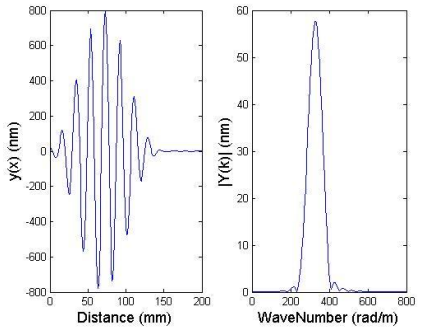

Figure IV.a - Distance and wavenumber curves for the out-of-plane displacement

In-plane load

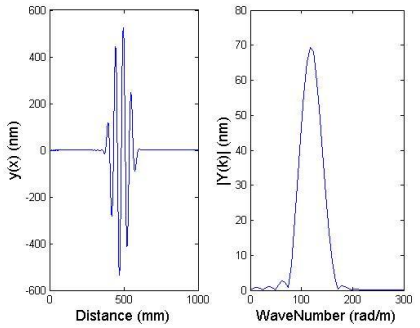

Figure IV.b - Distance and wavenumber curves for the in-plane displacement

A.5. 2D-FFT

Figures 7.a and 7.b allow showing the frequency and the wave number in the same graphics. While Figures 2 and 3 are obtained by a 1D FFT (Fast Fourier Transform), those one are obtained by a 2D FFT. These 2D FFT are corrects according to the theory: only one mode is propagating for each load and comparison with dispersion curves proves that they correspond exactly to the A0 and S0 modes.

Out-of-plane load

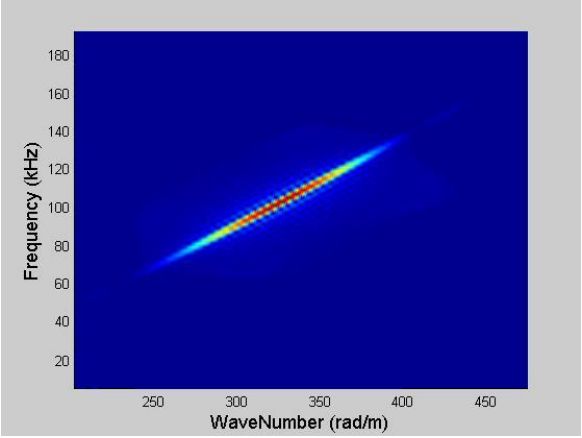

Figure V.a – Antisymmetric Mode 2D FFT

In-plane load

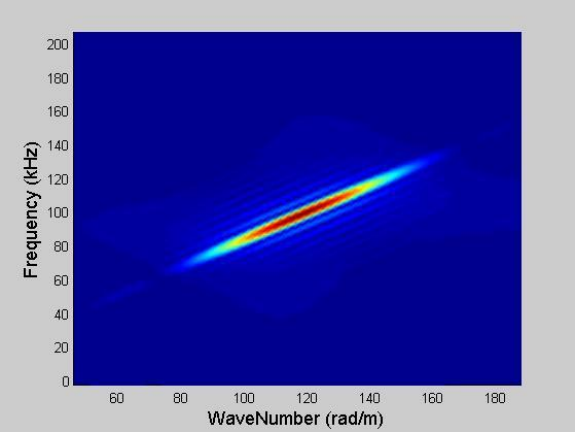

Figure V.b - Symmetric Mode 2D FFT

Moreover, it is possible to create two new graphics in extracting maximum value of wavenumber for each frequency. Figure 8 allows showing the value of wavenumber for a range of frequency for the A0 mode. Figure 9, the dispersion curve, proves that the simulation is correct, the solid line corresponds to the theoretical solution and the o-line corresponds to the ABAQUS solution.

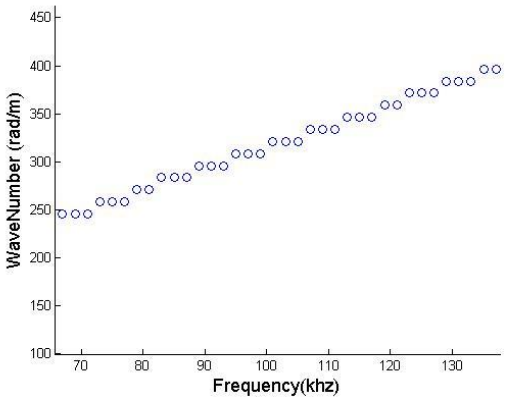

Figure VI – Wave number against frequency for the A0 Mode

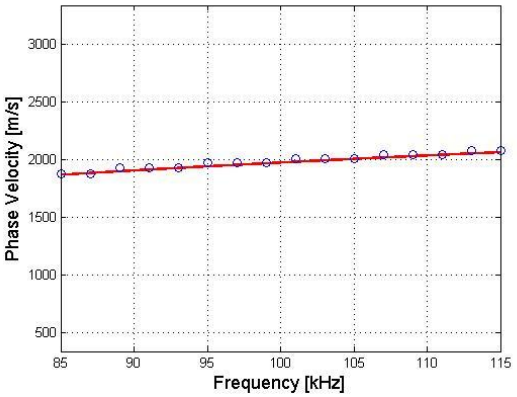

Figure VII – Phase velocity against frequency for the A0 Mode

B. PICTURES EXPLAINING ABAQUS PROGRAM

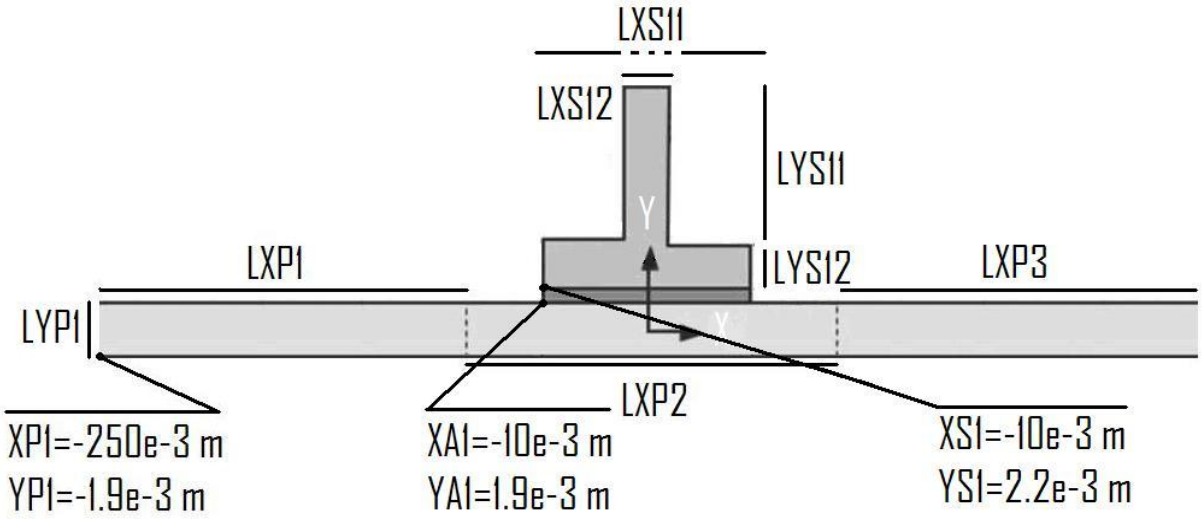

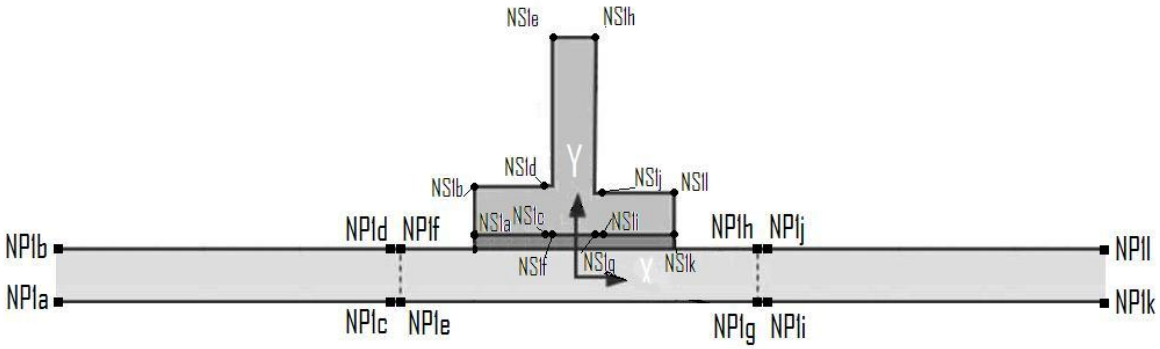

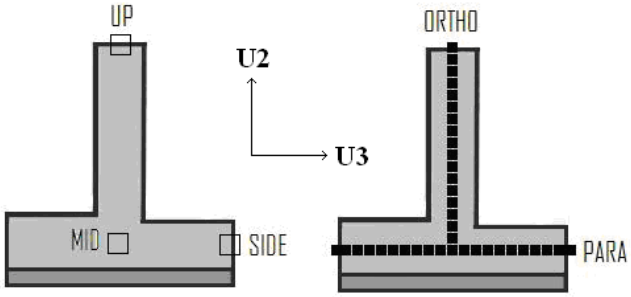

C. 2D FFT – PART III

A. SIMULATION 1

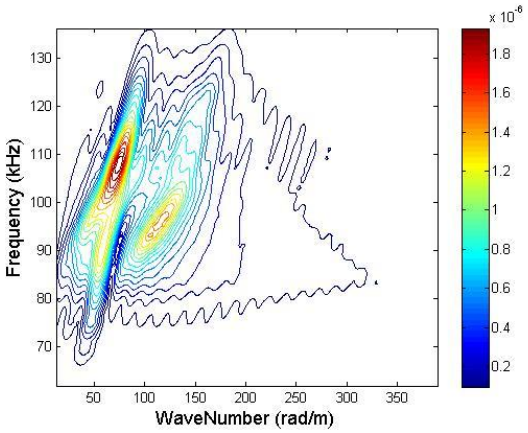

Figure VIII – 2D FFT – UP – U2

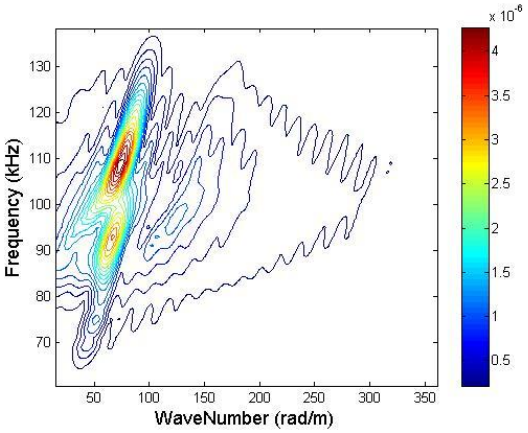

Figure VIII – 2D FFT – UP – U3

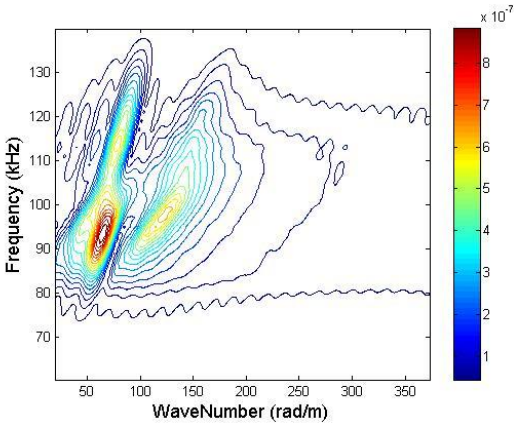

Figure VIII – 2D FFT – MID – U2

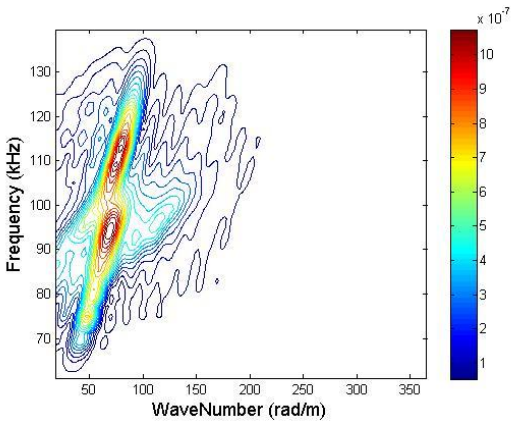

Figure VIII – 2D FFT – MID – U3

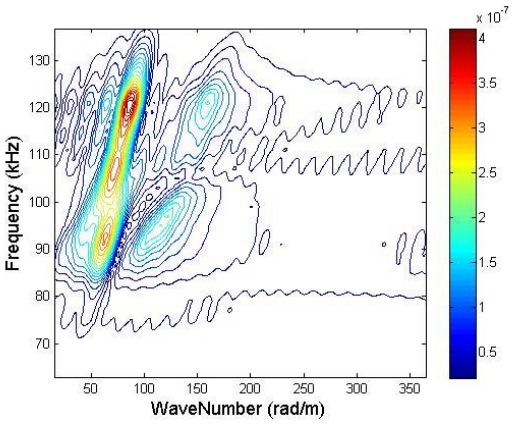

Figure VIII – 2D FFT – SIDE – U2

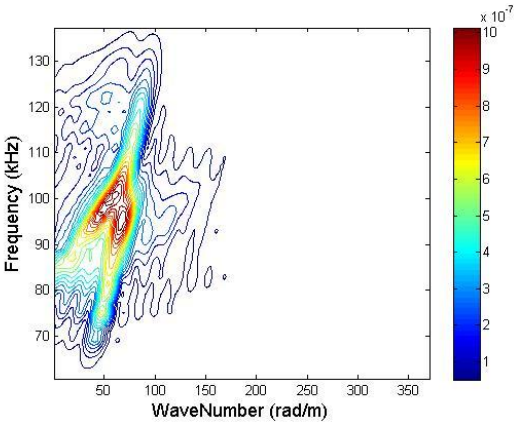

Figure VIII – 2D FFT – SIDE – U3

B. SIMULATION 2

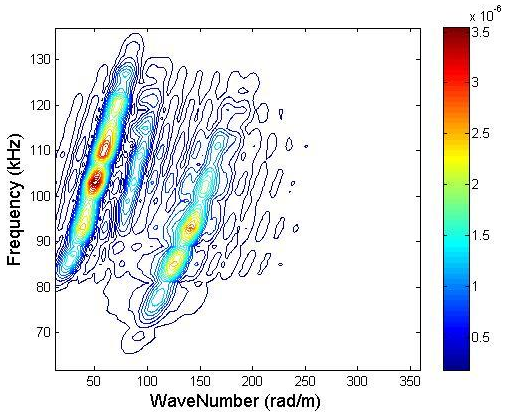

Figure IX – 2D FFT – UP – U2

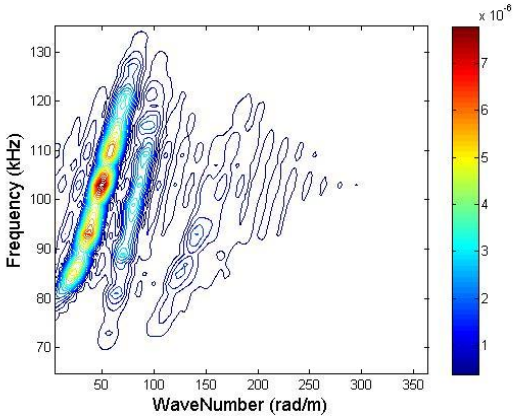

Figure IX – 2D FFT – UP – U3

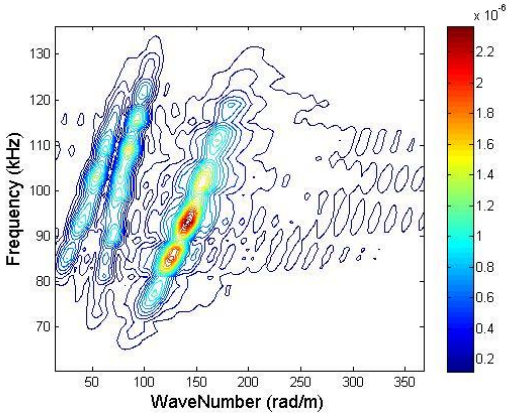

Figure IX – 2D FFT – MID – U2

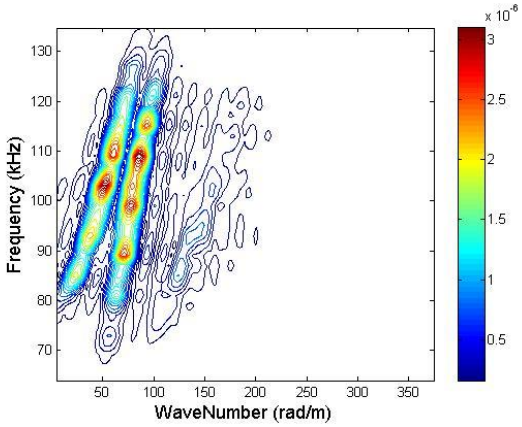

Figure IX – 2D FFT – MID – U3

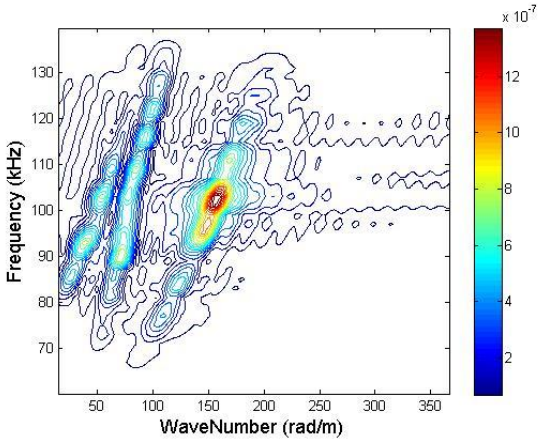

Figure IX – 2D FFT – SIDE – U2

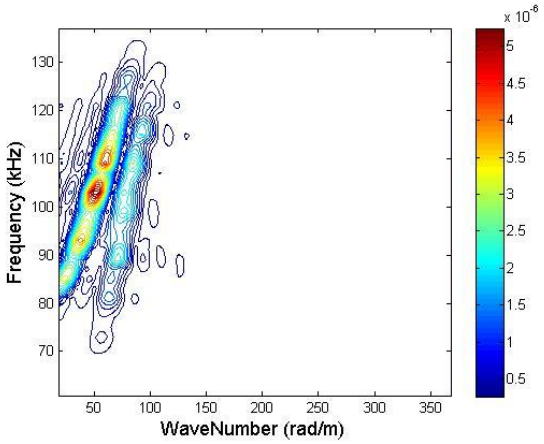

Figure IX – 2D FFT – SIDE – U3

C. SIMULATION 3

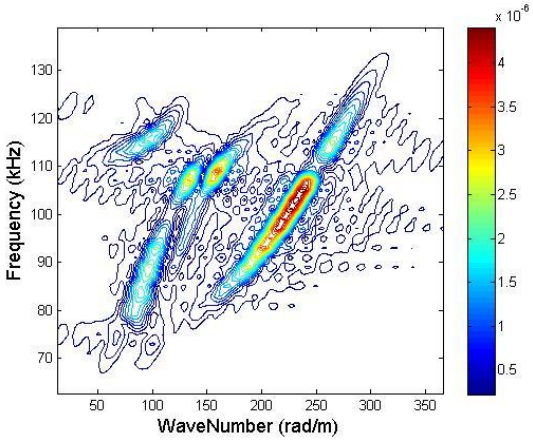

Figure X – 2D FFT – UP – U2

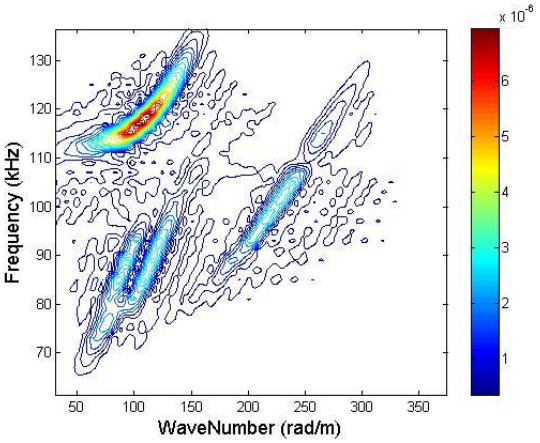

Figure X – 2D FFT – UP – U3

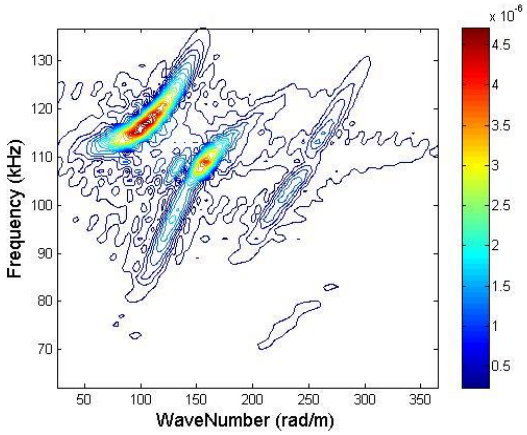

Figure X – 2D FFT – MID – U2

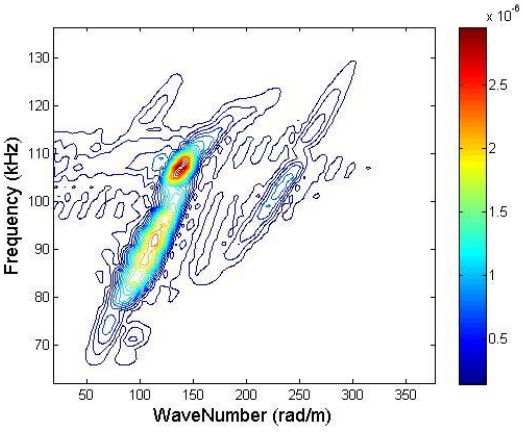

Figure X – 2D FFT – MID – U3

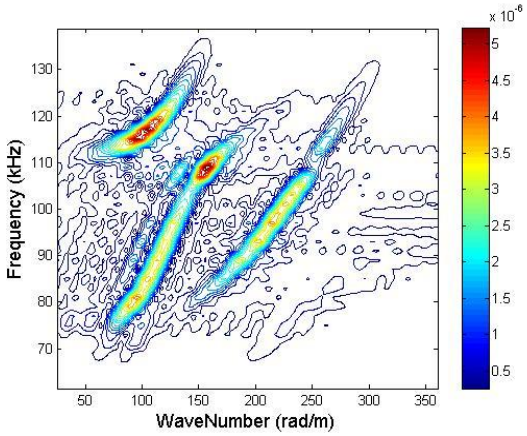

Figure X – 2D FFT – SIDE – U2

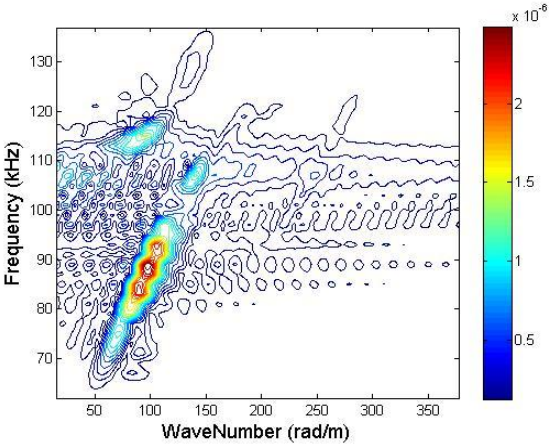

Figure X – 2D FFT – SIDE – U3

PART 2

RESEARCH INTO ULTRASONIC HORN

I. INTRODUCTION

Needles have always been used for immunisation and drug delivery however an alternative exists: low frequency ultrasound. Using ultrasound could increase drug delivery. One of the possibilities of this increase is that using ultrasound causes transient cavitations created by collapsing bubbles. A horn is used to create the inertial cavitation. Vibrations from the transducer are intensified by the horn, creating pressure waves. This action forms microscopic bubbles which expand and implode violently. Previous subject[1] had been studied including the mean to increase drug delivery through human nail tissue.

However, nobody knows the amplitude of the top of the horn. In fact, in the internet site of the manufacturer[2], it is written that the maximum amplitude of the transducer is 15 micrometers and that for this amplitude the horn's amplitude is 124 micrometers, so a ratio of 8.27. However, user can chose a percentage of this amplitude but doesn't know the exact value of the horn's amplitude.

In this part, the horn will be referred as the "ultrasonic horn", "horn" or "probe". Moreover, the amplitude of the top of the horn is the horn's amplitude and the amplitude of the transducer is the excitation's amplitude or load amplitude.

This project has two parts which final aim is to check if the results match between these two parts:

- Theoretical: modelling of the ultrasonic horn
- Experimental: measure of its amplitude with a laser vibrometer.

II. MODELLING OF THE HORN

1. Geometry, loads and monitoring points

The horn was measured and reproduced with ABAQUS CAE. Figure 1 shows that the ABAQUS model seems not too bad in accordance with the horn's picture.

The horn is made of Titanium 6Al-4V, which properties[3] are:

E=114GPa, v=0.342 and ρ=4.47 g/cm^3.

(E: Young's modulus, v: Poisson's ratio, ρ: density)

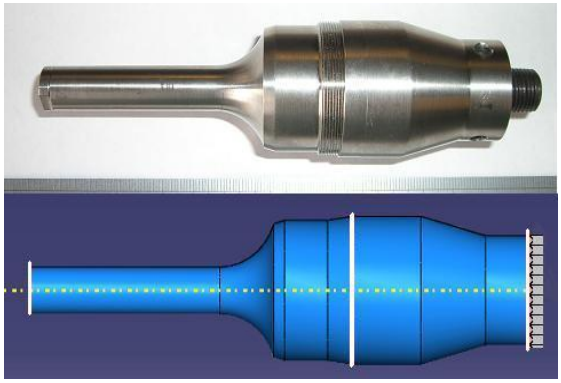

Figure 1. Comparison between the real horn and the horn designed by CAE.

Monitoring points are placed in front of the horn, in back of the horn and in the middle of the horn like shown, in white, figure 1.

The excitation is a sinusoidal in-plane displacement (BC command in ABAQUS) with a frequency of 20 kHz. It is applied on the back of the horn as figure 15 shown.

Stress-free conditions are defined at all outer limits of the system.

2. Results

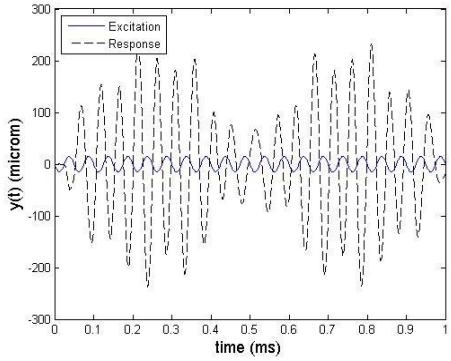

Figure 2 – Time traces for the excitation amplitude and for the horn's amplitude

In order to be able to compare the modelling results and the experiment results, the horn's amplitude was compared with the load amplitude.

Figure 2 shows the time traces for the excitation amplitude and for the horn's amplitude. It is obvious that the amplitude of the horn is multiplied in comparison with the amplitude of the excitation. However, the ratio between the two amplitudes is not constant compared to the time and this is not normal according to the manual.

Figure 3.a shows that the excitations' signal has a frequency of 20 kHz whereas figure 3.b shows that the signal at the top of the horn has 2 main frequencies. However, the signal at the top of the horn should have, according to the manual, a frequency of 20 kHz. Moreover, the horn's amplitude is not correct according to the manual (horn's amplitude should be 124 micrometers)

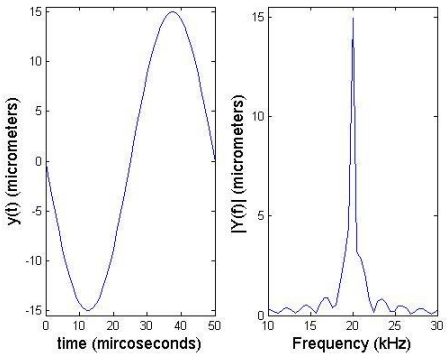

Figure 3.a - Amplitude and Frequency signal curves of the excitation

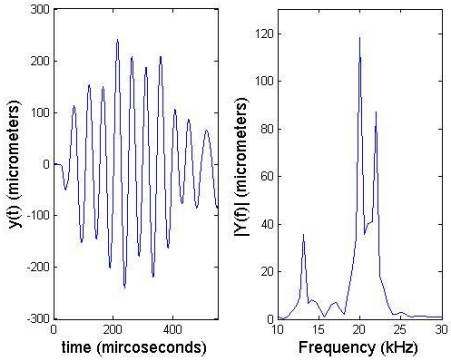

Figure 3.b - Amplitude and Frequency signal curves of the horn

The problem could be that the horn designed by ABAQUS is not exactly the same as the real one, and then the frequency resonance could not be the same. However, one doesn't know the real horn's amplitude. So, before continuing the ABAQUS's study, experiments was made to measure the horn's amplitude.

III. EXPERIMENTAL DETERMINATION OF THE AMPLITUDE.

1. Objectives, apparatus and experimental process

The main purpose of these experiments was to characterise the amplitude of the ultrasonic horn. The ultrasonic horn had been designed to operate in a liquid medium but it could be interesting to check if the horn can oscillate without being immersed in a liquid. So, the first experiment was the measurement, without immersion in a liquid, of the ultrasonic horn's amplitude.

The following apparatus was used to conduct these experiments:

- Ultrasonic horn: VCX 500 manufactured by "Sonics & Materials Inc". The horn is designed to resonate at 20 kHz. The horn is controlled by a box which allows changing the amplitude setting.
- The displacement is measured using a laser interferometer: OFV-505 manufactured by "Polytech".

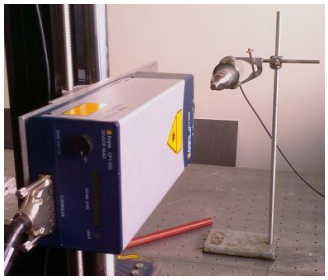

Figure 4. Apparatus

The exact procedure followed when carrying out these experiments is as follow:

- The laser is positioned to measure the amplitude at the top of the horn. It is then set avoiding having a maximum value of signal-to-noise ratio.
- The amplitude of the probe is set using the VCX's control box.
- The horn is started and the signal is capturing by the computer.

2. Results, observations and error analysis

The main interesting result is to check if the excitation and the signal at the top of the probe are at 20 kHz. Then, it is interesting to check if the amplitude given by the manual is correct. Figure 5.a shows the amplitude and the frequency curves of the transducer and the figure 5.b shows the amplitude and frequency curves of the signal on the top of the probe.

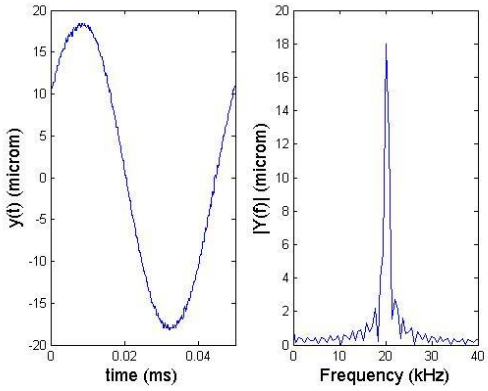

Figure 5.a - Amplitude and Frequency signal curves of the excitation

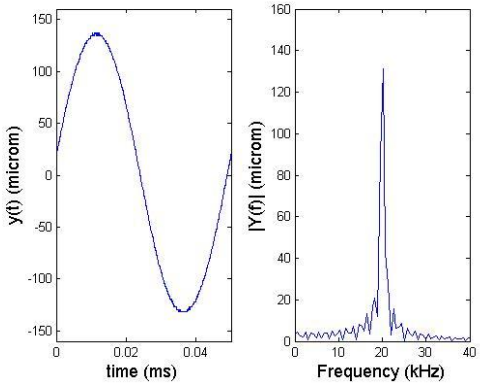

Figure 5. b - Amplitude and Frequency signal curves of the horn

Both frequencies curves show that the two signals are at 20 kHz. So, the first conclusion is that the ABAQUS model is wrong. Moreover, the amplitude of the excitation signal is at 18 micrometers which correspond to the value of 15 micrometers written in the manual (In fact, this amplitude depends on the Young Modulus of the Titanium). Furthermore, the horn's amplitude is at about 131 micrometers which correspond to the manual.

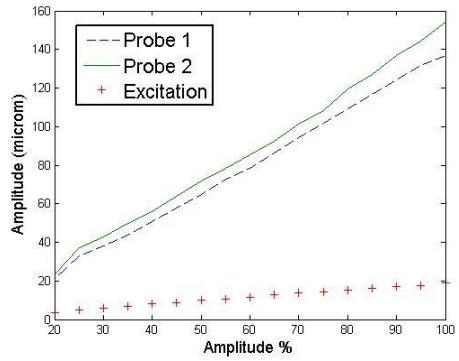

Figure 6 - Parametric trace of horns' amplitude and excitation amplitude

The second thing which is interesting to see is if the increasing of the horn's amplitude is linear, quadratic or exponential compared to the increase of the transducer's amplitude. Moreover, a second probe (probe 2 – figure 6), which is different because of a removal tip at the top of it, is compared to check differences between our two horns. A parametric study was done, measuring amplitude of the two horns and the transducer for different percentage of amplitude on the device.

According to figure XX, it is obvious that the amplitude increase linearly. However, the linearity coefficient is not the same for the excitation curve than for the horn curve and the ratio between the two coefficients is about 10.

To finish, some other measurements were done: the measurement at different points of the top of the horn and at different point of the excitation surface. The result is that the amplitude is the same on the entire surface.

In ABAQUS model, radial amplitude's shape is not the same at different time (Figure 7). However, the place of the maximum and the minimum is at the same place and measurements show showed that the ratio between horn's amplitude and radial amplitude doesn't exceed 2% whereas it is 5% with the simulation.

An experiment has been done to see effects of water on horn's amplitude with a tube around the top of the horn – figure 8 - to retain water; however it didn't work because the water evaporates immediately after contact with the horn. A better experiment could be done with a special apparatus[1].

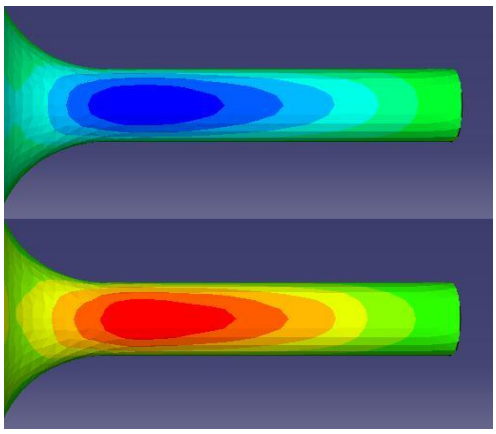

Figure 7 – Out-of-Plane amplitude (blue: minimum / red: maximum)

So, measurements show that data given in the manual are correct. However, experiments have not the same result as the ABAQUS simulation.

Figure 8 – Photo of the horn + tube

As said before, the problem could come from the fact that the horn is not well designed but it could come from the fact that the excitation is not the same. So, to check this aspect, a new simulation was done replacing the excitation file obtained by the one obtain by measurement of the transducer amplitude.

3. New simulations with the excitation file obtained by measurement

To complete this study, simulations were done with ABAQUS using the excitation file obtained by measurements. Unfortunately, the results are identical; the horn's amplitude is not constant and very different compared to the measurement's results.

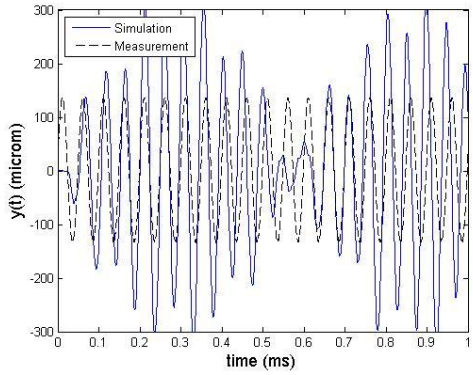

Figure 9 – Time traces of horn's amplitude obtained with the same excitation.

Figure 9 shows the horn's amplitude for the simulation and the measurement. This is obvious that the result is very different.

However, the load is not well modelled, in fact, there is a screw on the horn which is not modelled (figures I,II,III). Moreover, the horn is in contact with the transducer which implies reflections which are not take into account in the model. So three simulations were done to check the influence of the screw and the transducer on the horn's amplitude (figure 10).

The result is that the three horn's amplitude are different so, the presence of the screw and the transducer is non negligible. Moreover, many different simulations were done, changing the geometry of the horn, changing the frequency of the load, however no simulations gave us correct results.

So, many possibilities could explain differences between simulation and experiment:

- Geometry: Is the horn homogeneous? What are real dimensions of the horn?
- Properties: What are real properties of the horn?

And, to our mind, the main one:

- Load: How well model the load?

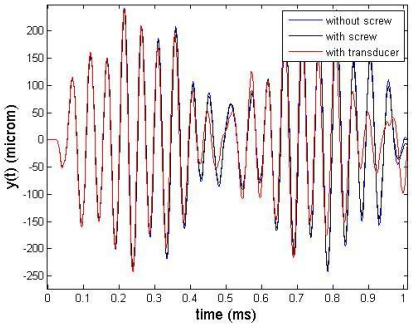

Figure 10 – Time traces of horn's amplitude.

To conclude, we saw that a little difference between two horns implies a non-negligible difference in horn's amplitude. So, the next step is to model with accuracy the horn and to take into account the presence of the transducer. So, it supposes to have real dimensions, properties and characteristic of horn and transducer which could be difficult to obtain because of, for example, difficulties to measure dimensions or manufacturing secret from "Sonics & Materials Inc".

4. Bibliography

[1]Favillier P.A, "Research into the use of ultrasound as a means of increasing drug delivery through human nail tissue", *Third Year Project*, UCL, 2008

[2]www.sonicsandmaterials.com/liquid-new-sheet/LargeVolAcess/ProbesandBoosters.pdf

[3]http://www.efunda.com/materials/alloys/titanium/show_titanium.cfm?ID=T18AB&prop=all&Page_Title=Ti-6Al-4V

APPENDIX

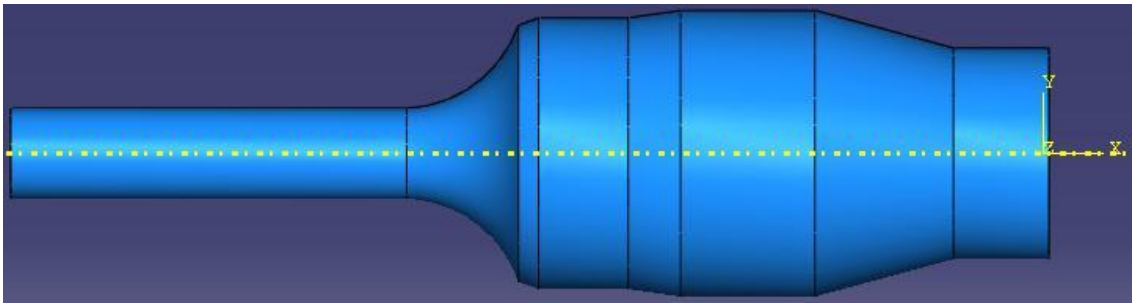

Figure I – ABAQUS's picture of the horn without screw

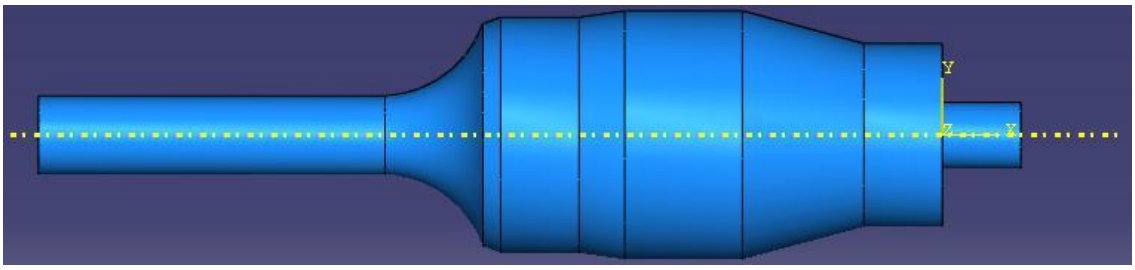

Figure II – ABAQUS's picture of the horn with screw

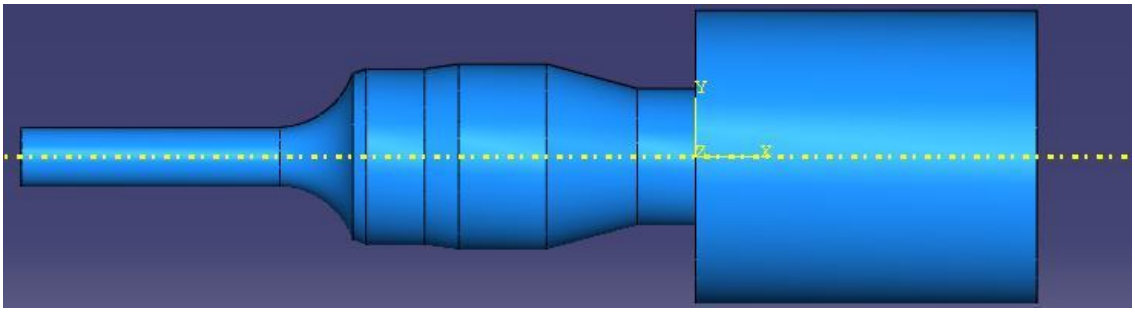

Figure III – ABAQUS's picture of the horn with screw and transducer

Summary

Engineering structures are subject to loads during service which can cause damage. Guided ultrasonic waves are investigated for the detection of defects as they propagate over larger distance in structures with limited access. ABAQUS model of a simple plate was validated by comparing to the theoretical results. The guided ultrasonic wave propagation in a three-dimensional model of a stiffener bonded to a plate has been studied and results have to be compared to COMSOL results and experimental results.

Needles have always been used for immunisation and drug delivery however an alternative exists: low frequency ultrasound. Using ultrasound could increase drug delivery. One of the possibilities of this increase is that using ultrasound causes transient cavitations created by collapsing bubbles. A horn is used to create cavitations by creating pressure waves. However, nobody knows the amplitude of the top of the horn. This project had two parts which final aim was to check if the results match between these two parts: Theoretical: modelling of the ultrasonic horn. Experimental: measure of its amplitude with a laser vibrometer. The experimental part confirmed the results given by the manual. However, the theoretical part with ABAQUS was not convincing and need a deeper study.

Résumé

Les structures complexes sont soumises à des efforts lors de leur utilisation ce qui abime la structure. Des ondes guidées sont utilisées pour la détection de défauts car elles se propagent sur de grandes distances dans des structures où l'accès est très complexe. Le model ABAQUS d'une plaque simple a été validé en comparant les résultats obtenus aux résultats théoriques. L'étude des ondes guidées dans un modèle en trois dimensions d'un raidisseur collé sur une plaque a été réalisée et les résultats doivent maintenant être comparés aux résultats obtenus avec COMSOL ainsi qu'avec les résultats expérimentaux.

Des aiguilles ont toujours été utilisées pour la vaccination ainsi que pour injecter des médicaments, cependant une alternative existe : l'utilisation d'ultrasons à basse fréquence. L'utilisation d'ultrasons permettrait de favoriser la pénétration du médicament dans le corps. Une des possibilités de cette augmentation est que l'utilisation d'ultrasons produit des cavités créées par l'effondrement de bulles sur elles-mêmes. Une sonde est utilisée pour créer les cavités en créant un champ de pression. Cependant, personne ne connait l'amplitude de cette sonde. Ce projet comprend donc deux parties, une partie théorique : la modélisation de la sonde et une seconde partie, expérimentale, qui consiste à en mesurer l'amplitude avec un vibromètre laser. La partie expérimentale a confirmé les résultats donnés par le manuel d'utilisation, cependant la partie théorique avec ABAQUS n'a pas été convaincante et une étude plus approfondie est nécessaire.